

TEMPORAL X-RAY RECONSTRUCTION USING TEMPORAL AND SPECTRAL MEASUREMENTS

F. Christie^{1,*}, J. Rönsch-Schulenburg, M. Vogt

Deutsches Elektronen-Synchrotron, 22607 Hamburg, Germany

Y. Ding, Z. Huang, J. Krzywinski, A. A. Lutman, T. J. Maxwell, D. Ratner

SLAC National Accelerator Laboratory, Menlo Park, California 94025, USA

V. A. Jhalani, California Institute of Technology, Pasadena, California 91125, USA

¹also at Universität Hamburg, 22607 Hamburg, Germany

Abstract

Transverse deflecting structures (TDS) are widely used in accelerator physics to measure the longitudinal density of particle bunches. When used in combination with a dispersive section, the whole longitudinal phase space density can be imaged. At the Linac Coherent Light Source (LCLS), the installation of such a device downstream of the undulators enables the reconstruction of the X-ray temporal intensity profile by comparing longitudinal phase space distributions with lasing on and lasing off [1]. However, the resolution of this TDS is limited to around 1 fs rms (root mean square), and therefore, in most cases, it is not possible to resolve single self-amplified spontaneous emission (SASE) spikes within one photon pulse.

By combining the intensity spectrum from a high resolution photon spectrometer [2] and the temporal structure from the TDS, the overall resolution is enhanced, thus allowing the observation of temporal, single SASE spikes. The combined data from the spectrometer and the TDS is analyzed using an iterative algorithm to obtain the actual intensity profile.

In this paper, we present the reconstruction algorithm as well as analyzed data obtained from simulations which shows the reliability of this method. Real data will be published at a later stage.

INTRODUCTION

The longitudinal phase space distribution of electron bunches can be mapped to transverse coordinates by streaking them using a transverse deflecting radio frequency (RF) structure (TDS) in one direction and combining that streak with a dipole magnet which serves as an energy spectrometer in the other direction. The beam can then be imaged using a screen station and the longitudinal phase space distribution can be reconstructed [3]. When the TDS is installed downstream of the undulators at a Free-Electron Laser (FEL) the X-ray temporal profile can be obtained by comparing images where the FEL process is suppressed to images where it is enabled [1, 4]. However, such a measurement is limited primarily by the resolution of the TDS, which is given by

$$R_t = \frac{\sqrt{\epsilon_u} \cdot pc}{\sqrt{\beta_u(s_0)} \cdot \sin(\Delta\Psi_u) \cdot eV_0\omega_{RF} \cdot \cos(\Phi_{RF})}, \quad (1)$$

* florian.christie@desy.de

with the geometric emittance ϵ_u in the deflecting plane u , the momentum of the electrons p , the speed of light c , the beta function at the TDS $\beta_u(s_0)$, the phase advance between the TDS and the screen $\Delta\Psi_u$, the elementary charge e , the deflecting voltage V_0 , the frequency of the RF ω_{RF} , and the RF phase Φ_{RF} . For a typical TDS used at an FEL, such as the Linac Coherent Light Source (LCLS), the resolution is limited to the order of 1 fs rms (root mean square). This leads to blurring of the intensity profile. Therefore, in most cases this measurement technique fails to resolve the spiky nature of the self-amplified spontaneous emission (SASE) process of an FEL. In addition to the temporal measurement using a TDS, the spectral domain of the emitted radiation can be measured using a spectrometer. Since the spectral and time domain are conjugated domains of the Fourier transform, we combine both to enhance the resolution of the actual intensity profile. For this, we introduce an iterative algorithm which is presented in this paper.

ITERATIVE RECONSTRUCTION ALGORITHM

To test the reconstruction algorithm, simulated data of the SASE process is analyzed. Both the spectral and the temporal profile are taken at the end of the linear regime prior to saturation. At saturation slippage significantly lengthens the photon pulse beyond the length of the lasing domain of the bunch.

We assume the temporal intensity profile $I(t)$ is blurred by the finite resolution of the TDS through a convolution with a Gaussian $G(t)$ of fixed width R_t

$$(I * G)(t) = \tilde{I}(t). \quad (2)$$

This blurred intensity profile $\tilde{I}(t)$ and the spectral intensity profile $\mathcal{I}(\omega)$, which we assume to have unlimited resolution for now, are the starting point for the reconstruction algorithm.

Gaussian Base Functions

First, we model the electric field as a sum of base functions in time. For now, we use the sum of Gaussians of fixed width σ_i centered at times t_i , with varying complex coefficients a_i

$$F(t) = \sum_i^n a_i B_i(t) = \sum_i^n a_i \left(\frac{1}{\sqrt{\pi}\sigma_i} \right)^{\frac{1}{2}} e^{-\frac{(t-t_i)^2}{2\sigma_i^2}} e^{i\omega_i t}, \quad (3)$$

the ω_i can be initially calculated based on the energy profile of the electron phase space. Otherwise, they are initialized as zero. The σ_i are chosen to be smaller than the expected width of the single SASE spikes. The t_i are chosen such that the system is not badly conditioned, yet single SASE spikes can be modeled. After a Fourier transform, we obtain the field in the frequency domain

$$\mathcal{F}(\omega) = \sum_i^n a_i \mathcal{B}_i(\omega) = \sum_i^n a_i \left(\frac{\sigma_i}{\sqrt{\pi}} \right)^{\frac{1}{2}} e^{-it_i(\omega-\omega_i)} e^{-\frac{\sigma_i^2(\omega-\omega_i)^2}{2}}. \quad (4)$$

The complex coefficients a_i are initialized randomly. Every a_{1+2n} coefficient has its amplitude reduced by 8, every a_{1+5n} reduced by 16, resulting in starting temporal and spectral intensity profiles consisting of a few wider spikes instead of frequent narrower spikes, thereby resembling the nature of SASE more. To match the integral of the blurred intensity profile, the coefficients are normalized so that $\int \tilde{I}(t) dt = \int |F(t)|^2 dt$. These normalized coefficients are then used to create the initial guess $F_0(t)$ and $\mathcal{F}_0(\omega)$.

Iteration Process and Minimizing

For the iteration process, we use the alternate projection method described in [5]. Since in general $|\tilde{F}_n(t)|^2 \neq \tilde{I}(t)$, at each iteration n , the previously calculated field $F_n(t)$ is projected on the blurred intensity profile $\tilde{I}(t)$. This is done by introducing the projected field

$$U_n(t) = F_n(t) \cdot \sqrt{\frac{\tilde{I}(t)}{|\tilde{F}_n(t)|^2}} \quad (5)$$

which keeps the complex phases of $F_n(t)$ and satisfies $|\tilde{U}_n(t)|^2 = \tilde{I}(t)$. Additionally, we calculate the projected spectrum

$$V_n(\omega) = \mathcal{F}_n(\omega) \cdot \sqrt{\frac{\mathcal{I}(\omega)}{|\mathcal{F}_n(\omega)|^2}}. \quad (6)$$

Since $U_n(t)$ and $V_n(\omega)$ can in general not be written in the form of Eqs. (3) and (4), we try to find a new field $F_{n+1}(t)$ and its transform $\mathcal{F}_{n+1}(\omega)$, that minimize the distance from the projections

$$d = \|F_{n+1} - U_n\|_{\mathcal{L}^2}^2 + \|\mathcal{F}_{n+1} - V_n\|_{\mathcal{L}^2}^2 \\ = \left\| \sum a_{i,n+1} B_i - U_n \right\|_{\mathcal{L}^2}^2 + \left\| \sum a_{i,n+1} \mathcal{B}_i - V_n \right\|_{\mathcal{L}^2}^2. \quad (7)$$

Using the \mathcal{L}^2 scalar product [6]

$$\langle a, b \rangle = \int_{-\infty}^{\infty} a(x)b^*(x)dx, \quad \langle a, a \rangle = \|a\|_{\mathcal{L}^2}^2 \quad (8)$$

we can rewrite Eq. (7)

$$d = \sum_i \sum_j a_{i,n+1} a_{j,n+1}^* \langle B_i, B_j \rangle + \|U_n\|_{\mathcal{L}^2}^2 \\ - \sum_i a_{i,n+1} \langle B_i, U_n \rangle - \sum_j a_{j,n+1}^* \langle U_n, B_j \rangle \\ + \sum_k \sum_l a_{k,n+1} a_{l,n+1}^* \langle \mathcal{B}_k, \mathcal{B}_l \rangle + \|V_n\|_{\mathcal{L}^2}^2 \\ - \sum_k a_{k,n+1} \langle \mathcal{B}_k, V_n \rangle - \sum_l a_{l,n+1}^* \langle V_n, \mathcal{B}_l \rangle. \quad (9)$$

d is minimized by finding $a_{i,n+1}$, so that the derivative of d with respect to all $a_{i,n+1}$ is equal to zero. After some simplifications and the application of the scalar product in Eq. (8), we obtain

$$\int U_n(t) B_k^*(t) dt + \int V_n(\omega) \mathcal{B}_k^*(\omega) d\omega = \sum_i^n a_{i,n+1} (T_{ik} + F_{ik}), \quad (10)$$

where $T_{ij} = \langle B_i, B_j \rangle$ and $F_{ij} = \langle \mathcal{B}_i, \mathcal{B}_j \rangle$. For the Gaussian base functions in Eqs. (3) and (4) this yields

$$T_{ij} = \sqrt{\frac{2\sigma_i\sigma_j}{\sigma_i^2 + \sigma_j^2}} \cdot e^{-\frac{(t_i-t_j)^2 - 2i(\omega_i-\omega_j)(t_i\sigma_j^2+t_j\sigma_i^2) + \sigma_i^2\sigma_j^2(\omega_i-\omega_j)^2}{2(\sigma_i^2+\sigma_j^2)}} \quad (11)$$

and $F_{ij} = T_{ij}$ due to the properties of the Fourier transform.

In each iteration step new coefficients $a_{i,n+1}$ are calculated according to Eq. (10). Using those coefficients, the temporal and the spectral field are calculated according to Eqs. (3) and (4) and are fed back into the iteration algorithm.

RESULTS

The iterative reconstruction algorithm is tested using simulations of the SASE process in the LCLS undulators at 1.5 nm, which are conducted using the leap-frog algorithm developed by Z. Huang [7]. To start, we simulate FEL pulses of bunches of 20 pC, 40 pC, and 150 pC charge, resulting in photon pulses of different length. These simulations are done using only one single random SASE seed per charge, resulting in only one intensity profile per charge. Further testing on the code is done using the intensity profiles of 50 different SASE shots right before saturation (using different initial seeds due to the statistical nature of SASE) for a charge of 40 pC. The temporal and spectral profile are taken at the end of the linear regime. The Gaussian blurrings used are in the range of 1.2 fs to 0.5 fs. For each shot 50 reconstructions using different initial base functions are carried out. To obtain the final reconstruction, these 50 reconstructions are then averaged. Figures 1 to 3 show the results for the different bunch charges: the blue solid line is the actual intensity profile from the simulation $I(t)$, the red solid line is the blurred intensity profile $\tilde{I}(t)$ using a resolution of $R_t = 1$ fs in these cases. The dashed lines are the results of the 50 reconstructions using different initial base functions. The black solid line is the mean of the 50 reconstructions

Content from this work may be used under the terms of the CC BY 3.0 licence (© 2018). Any distribution of this work must maintain attribution to the author(s), title of the work, publisher, and DOI.

surrounded by a light gray shaded area that is one standard deviation.

To determine how well the algorithm reconstructs the actual intensity profile the $1 - R^2$ value known from statistics [8, 9] is used

$$1 - R^2 = \frac{\sum_{i=1}^n (y_i - \hat{y}_i)^2}{\sum_{i=1}^n (y_i - \bar{y})^2}. \quad (12)$$

The sum $\sum_{i=1}^n (y_i - \bar{y})^2$, where the y_i are the observed data with their mean value \bar{y} , is called the total sum of squares and can be described as the total variation of the actual y_i values about their mean \bar{y} [9]. The sum $\sum_{i=1}^n (y_i - \hat{y}_i)^2$, where the \hat{y}_i are the predicted data, is called the residual sum of squares, since it is the residual or unexplained variation of the y_i values about the predicted values \hat{y}_i [9]. A $1 - R^2$ value of zero means a perfect agreement. In our case y is the actual intensity profile $I(t)$ and \hat{y} is the obtained reconstructed intensity profile $F(t)$.

As can be seen at the top of Figs. 1 to 3, the algorithm is able to retrieve the actual intensity profile of the single shots with $1 - R^2 = 0.04$ for the 20 pC simulation, $1 - R^2 = 0.17$ for the 40 pC simulation, and $1 - R^2 = 0.11$ for the 150 pC simulation, respectively. The main features of the photon pulse intensity profile can be reconstructed. Smaller adjacent spikes are more difficult to reconstruct, as they are washed out too strongly by the resolution of the TDS.

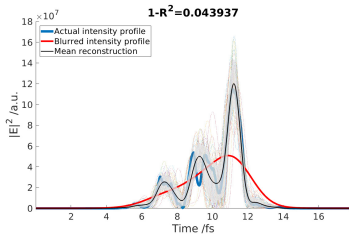


Figure 1: Reconstruction for 20 pC, $R_t = 1$ fs.

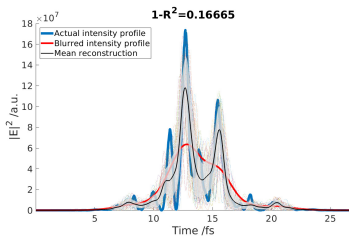


Figure 2: Reconstruction for 40 pC, $R_t = 1$ fs.

Figure 4 shows again the photon pulse from the simulated bunch with 40 pC. In this case, the Gaussian blurring used is 0.5 fs. As can be seen, even for such a high resolution, the blurred profile still looks very different from the actual profile, but the reconstruction is now able to resolve even the smaller side peaks.

The $1 - R^2$ value for the 50 different shots using different initial seeds and the different resolutions R_t can be found in Fig. 5. For a TDS resolution of 0.5 fs the $1 - R^2$ values

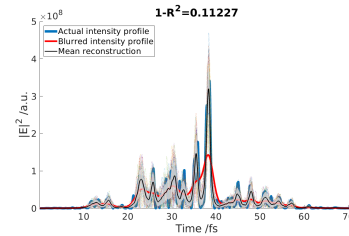


Figure 3: Reconstruction for 150 pC, $R_t = 1$ fs.

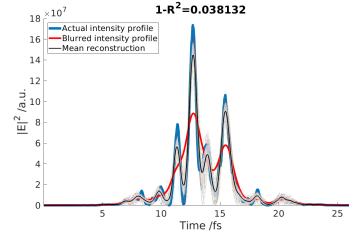


Figure 4: Reconstruction for 40 pC, $R_t = 0.5$ fs.

of all reconstructions are in the order of 0.1. If we assume a TDS resolution of 0.75 fs, the most $1 - R^2$ values are in the region of 0.1 to 0.2, and there are a couple of shots with $1 - R^2$ in the order of 0.3. For resolutions of 1 fs and 1.2 fs most of the shots can still be reconstructed with a $1 - R^2$ value between 0.1 and 0.3. A small number of shots for a resolution of 1.2 fs are reconstructed with a $1 - R^2$ value in the region of 0.3 to 0.4. As can be also seen in Fig. 5 the $1 - R^2$ value for the same resolution varies from shot to shot for the 50 different seeds. This indicates that the $1 - R^2$ value does not depend on the charge, but rather on the complexity of the intensity profile. Small, frequent, adjacent spikes are harder to reconstruct than a few separated spikes.

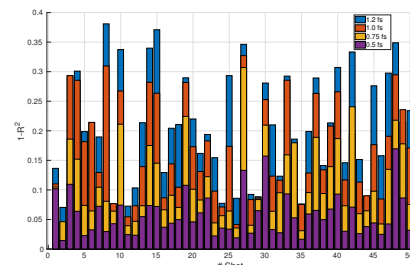


Figure 5: Results of the reconstruction of 50 different SASE shots for different TDS resolutions. The $1 - R^2$ value is plotted against the shot number.

SUMMARY

In this paper, we introduced an iterative reconstruction algorithm and showed that it is able to reconstruct the temporal intensity profile of a SASE pulse by combining blurred temporal and spectral intensity profiles. The accuracy of the reconstruction depends on the TDS resolution. For example, to reconstruct all SASE spikes for the 40 pC case a TDS resolution of $R_t = 0.5$ fs is needed. Experimental data will be published in due course.

REFERENCES

- [1] Y. Ding *et al.*, “Femtosecond X-ray pulse temporal characterization in free-electron lasers using a transverse deflector”, *Phys. Rev. ST AB*, vol. 14, p. 120701, 2011.
- [2] D. Zhu *et al.*, “A single-shot transmissive spectrometer for hard X-ray free electron lasers”, *Appl. Phys. Lett.*, vol. 101, p. 034103, 2012.
- [3] P. Emma, J. Frisch, and P. Krejcik, “A Transverse RF Deflecting Structure for Bunch Length and Phase Space Diagnostics”, Stanford, CA, USA, Rep. LCLS-TN-00-12, Aug. 2000.
- [4] J. Bødewadt *et al.*, “Experience in operating sFLASH with high-gain harmonic generation”, in *Proc. IPAC'17*, Copenhagen, Denmark, May 2017, paper WEPAB016, pp. 2596–2599.
- [5] L.G. Gubin, B.T. Polyak, and E.V. Raik, “The method of projections for finding the common point of convex set”, *USSR Comp. Math. and Math. Phys.*, vol. 7, no. 6, pp. 1–24, 1967.
- [6] O. Forster, *Analysis 3*. Wiesbaden, Germany: Springer Spektrum, 2017.
- [7] K.-J. Kim, Z. Huang, and R. Lindberg, *Synchrotron Radiation and Free-Electron Lasers*. Cambridge, United Kingdom: Cambridge University Press, 2017.
- [8] H.-J. Mittag, *Statistik: eine Einführung mit interaktiven Elementen*. Berlin, Germany: Springer Spektrum, 2014.
- [9] D.N. Gujarati, *Basic Econometrics*. Boston, MA, United States: McGraw Hill, 2003.